Original Article

대한치과재료학회지 52(2) : 55-66, 2025
Korean Journal of Dental Materials (*Korean J Dent Mater*)
ISSN:2384-4434 (Print); 2384-3268 (Online)
Available online at http://www.kadm.org
http://dx.doi.org/10.14815/kjdm.2025.52.2.55

Taguchi 실험계획법과 임피던스 분석을 이용한 MTA 조성 최적화 연구

한미경[1], 송선주[2], 박영준[1,*]

[1]전남대학교 치의학전문대학원 치과재료학교실
[2]전남대학교 공과대학 신소재공학부

Optimization of mineral trioxide aggregate formulation using Taguchi design and impedance analysis

Mi-Kyung Han[1], Sun-Ju Song[2], Yeong-Joon Park[1,]*

[1]Department of Dental Materials, School of Dentistry, Chonnam National University, Gwangju 61186, Korea
[2]Department of Materials Science and Engineering, Chonnam National University, Gwangju 61186, Korea

MTA (mineral trioxide aggregate)는 우수한 생체적합성과 밀폐성을 지님에도 불구하고 조작의 불편함과 긴 경화 시간으로 인해 임상 적용에 제한이 있다. 본 연구는 다꾸찌(Taguchi) L9 (3^4) 직교 배열을 활용하여 MTA의 주요 구성 성분인 삼칼슘실리케이트(C3S), 이칼슘실리케이트(C2S), 삼칼슘알루미네이트(C3A), 그리고 물-시멘트비(W/C 비율)가 경화 시간에 미치는 영향을 분석하고, 최적 조성 조건을 도출하고자 하였다. C3S, C2S, C3A는 고상법으로 합성하였으며, XRD, SEM, DSC 분석을 통해 구조적 및 물리적 특성을 평가하였다. 수화 반응 중 임피던스 분석을 통해 각 성분의 수화 특성과 경화 진행을 모니터링하였고, 최적 조건(C3S: 2, C2S: 1, C3A: 3, W/C: 0.3)으로 제조한 시멘트를 입자 크기별(≤38 μm, 38-75 μm, >75 μm)로 분류하여 경화 시간을 측정한 결과, 입자가 작을수록 경화 시간이 단축됨을 확인하였다. 최적 조건을 적용한 시멘트는 가장 미세한 입자 그룹에서 약 41분의 경화 시간을 보였다. 본 연구는 MTA의 경화 시간 제어를 위한 효과적인 접근법을 제시하며, 고기능성 치과용 시멘트 개발을 위한 기초 자료로 활용될 수 있을 것이다.

색인단어 : 칼슘실리케이트 시멘트, 다꾸치 실험계획법, 임피던스 분석, 경화시간

Introduction

Since its introduction in 1993 under the brand name ProRoot® MTA (Dentsply Tulsa Dental, Johnson City, TN, USA), mineral trioxide aggregate (MTA) has become an widely used material in endodontic and restorative dentistry. Its clinical applications include root canal sealing, pulp capping, pulpotomy, apexification, perforation repair, and apical sealing (1, 2). MTA is favored for its excellent biocompatibility, non-toxicity, reliable sealing ability even under moist conditions, and dentin bridge formation (3). It is primarily composed of Portland

Sun-Ju Song (ORCID ID: 0000-0002-5518-1633)
Mi-Kyung Han (ORCID ID: 0000-0003-1434-1562)

*Correspondence: Yeong-Joon Park (ORCID ID: 0000-0003-0382-8535)
77, Yongbong-ro, Buk-gu, Gwangju 61186, Korea
Affiliation: Department of Dental Materials, School of Dentistry, Chonnam National University, Gwangju 61186, Korea
Tel: +82-62-530-4871, Fax: +82-62-530-4875
Email: yjpark@jnu.ac.kr

Received: May. 29, 2025; Revised: June. 18, 2025; Accepted: June. 19, 2025

cement and bismuth oxide (as a radiopacifier), typically mixed at a 4:1 ratio (4). The major functional components of MTA, tricalcium silicate (C3S) and dicalcium silicate (C2S), react with water to form calcium silicate hydrate (C-S-H) and calcium hydroxide (CH). The C–S–H contributes to mechanical strength and dimensional stability, while CH provides high alkalinity (pH ~12.5), promoting antibacterial effects and hard tissue formation (5).

Gray MTA (GMTA), the original formulation, contains aluminoferrite, which contributes to discoloration. In 2002, white MTA (WMTA) was developed by removing this component to enhance aesthetics (6, 7). WMTA exhibits a significantly shorter setting time (~15 min) compared to the 2-4 h required for conventional GMTA (8). However, due to its smaller and narrower particle size distribution (eight times smaller than GMTA), some studies have reported that WMTA is more challenging to work with than GMTA (9).

Numerous commercial MTA products have been introduced over the years. Despite these advancements, MTA continues to face limitations such as high cost, handling difficulty, and long setting time, restricting its widespread application (10). To address these issues, various approaches have been explored, including the use of additives such as calcium chloride, sodium lactate, and propylene glycol, and the development of improved delivery systems (11, 12). However, many of these efforts have relied on empirical, trial-and-error approaches, lacking a systematic investigation of how individual component ratios affect performance.

The Taguchi L9 (3^4) orthogonal array design provides a statistically robust and efficient method to evaluate the effects of multiple variables with a limited number of experiments. This method has been widely used in materials research to identify key compositional factors influencing physical properties (13). Applying this approach to MTA enables a structured optimization of formulation by examining the influence of C3S, C2S, tricalcium aluminate (C3A), and the water-to-cement (W/C) ratio on setting behavior. Furthermore, electrochemical impedance spectroscopy (EIS) was used to monitor the hydration process and determine setting time with precision. EIS is a non-destructive, real-time analytical technique that captures the evolution of electrical resistance during hydration, making it well suited for evaluating the dynamic setting behavior of cementitious systems.

In this study, the major components of C3S, C2S, and tricalcium aluminate (C3A) were individually synthesized using a solid-state method. Their structural and physicochemical characteristics were characterized using XRD, SEM, and DSC. Impedance analysis was performed to monitor the hydration process, and additional characterization was conducted after halting hydration with acetone. Using the Taguchi L9 design, this study systematically evaluated the influence of key compositional factors and W/C ratio on setting time. This study provides a systematic and efficient approach for controlling the setting time of MTA, providing foundational insights for the development of high-performance dental materials.

Materials and Methods

Reagent-grade raw materials were used to synthesize the cement components, including CaO (99.95%), SiO_2 (99.9%), Al_2O_3 (99%), MgO (99+%), Na_2CO_3 (99.5%), CaF_2 (99.5%), Bi_2O_3 (99.9%), and $CaSO_4 \cdot 2H_2O$ (99%), all of which were purchased from Alfa Aesar. The compositions for synthesizing tricalcium silicate (C3S), dicalcium silicate (C2S), and tricalcium aluminate (C3A) are listed in Table 1. The raw materials were weighed accordingly, mixed with isopropyl alcohol (IPA), and homogenized using a ball mill for over 24 h. The resulting slurry was dried at 80 ℃ for 24 h, followed by calcination in a platinum

Table 1. Composition of starting materials for synthesizing C3S, C2S, and C3A

Component / Ingredients	C2S	C3S	C3A
CaO, g	5.61	8.41	8.41
SiO_2, g	3.00	3.01	-
Al_2O_3, g	-	-	5.10
MgO, g	0.06 (0.7%)	0.17 (0.7%)	0.14 (0.7%)
Na_2CO_3, g	0.03 (0.3%)	0.03 (0.3%)	0.41 (3%)
CaF_2, g	-	0.06 (0.5%)	-
Bi_2O_3, g	0.26 (3%)	-	-

Table 2. Experimental factors and levels using Taguchi L9 (3^4) orthogonal array

Level / Factor	1	2	3
A. C2S	25%	50%	75%
B. C3S	25%	50%	75%
C. C3A	25%	50%	75%
D. W/C	0.3	0.5	0.7

crucible at designated temperatures: 1150 ℃ for C2S, 1450 ℃ for C3S, and 1400 ℃ for C3A, each for 5 h. The samples were then rapidly cooled.

The synthesized powders were characterized using X-ray diffractometry (XRD; D/Max Ultima III, Rigaku, Japan) and scanning electron microscopy (SEM; JSM-7900F, JEOL, Japan). The heat evolution during hydration was evaluated by differential scanning calorimetry (DSC; DSC3, Mettler Toledo, Switzerland). Setting behavior was analyzed using electrochemical impedance spectroscopy (EIS) with a frequency response analyzer (SI-1260, Solatron, UK). Impedance spectra were acquired using Z60 software, over a frequency range from 10^6 Hz to 0.1 Hz, with 10 points per decade on a logarithmic scale.

To systematically evaluate the influence of C3S, C2S, C3A content, and the water-to-cement (W/C) ratio on MTA setting time, a Taguchi L9 (3^4) orthogonal array design was employed (13). The factors and their corresponding levels are listed in Table 2.

Results

1. X-ray diffraction and microstructure of the synthesized MTA components

X-ray diffraction (XRD) analysis was performed to verify the phase purity of the synthesized MTA components-C3S, C2S, and C3A. The diffraction patterns shown in Figures 1(a), 1(b), and 1(c) correspond to monoclinic C3S (JCPDS # 860402), β-C2S (JCPDS # 860398), and cubic C3A (ICDD # 38-1429), respectively, confirming the successful synthesis of single-phase structures (14). Minor secondary peaks

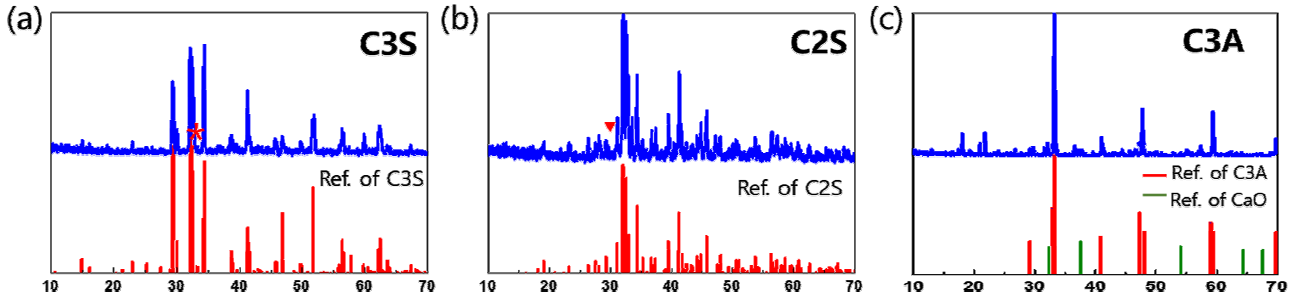

Figure 1. XRD patterns of synthesized C3S, C2S, and C3A powders.

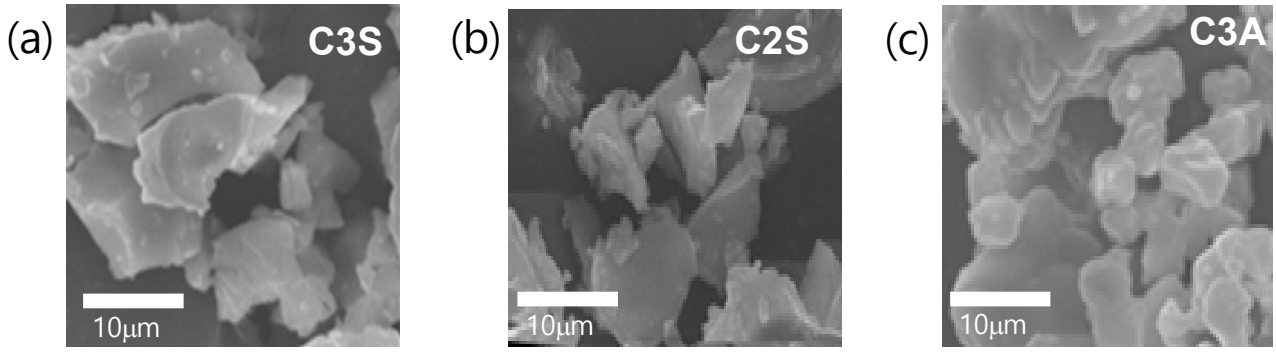

Figure 2. SEM images of synthesized C3S, C2S, and C3A powders.

were observed in the C3S and C2S patterns at 2θ = 32.1° and 34.4°, indicating trace coexistence of C2S and C3S (denoted by* and ▼). In the C3A pattern, additional peaks suggest the coexistence of approximately 11% CaO impurities (ICDD card #37-1497). These impurities may affect the initial and intermediate setting behavior of the cement (15). Therefore, optimizing the synthesis conditions is essential to minimize the formation of such secondary phases.

The microstructures of C3S, C2S, and C3A were examined using scanning electron microscopy (SEM), as shown in Figure 2. All synthesized powders exhibited irregular, plate-like morphologies, and the particle sizes were found to be approximately below 30 μm.

2. Differential scanning calorimetric analysis

Differential scanning calorimetry (DSC) was conducted to evaluate the hydration behavior of the synthesized powders over a 120-min period, as shown in Figure 3. The initial peak in the heat flow curve corresponds to the dissolution of cement particles upon mixing with water (16). The induction period of cement hydration of C3S is slower compared to C2S and C3A. The cumulative heat curves of C3S and C2S exhibit a rapid exothermic reaction within the first 10 min, reflecting the formation of calcium silicate hydrate (C-S-H) and calcium hydroxide (CH), with continued heat release up to 80 min, suggesting sustained hydration and strength development (17). In contrast, C3A reacted rapidly, completing its exothermic reaction within approximately 20 min due to the formation of calcium aluminate hydrate (C–A–H), which contributes to early-stage strength development of the cement (18). These results highlight the functional distinction among the components: C3A plays a critical role in initiating early setting and strength gain, while C3S and C2S contribute to the prolonged hydration process essential

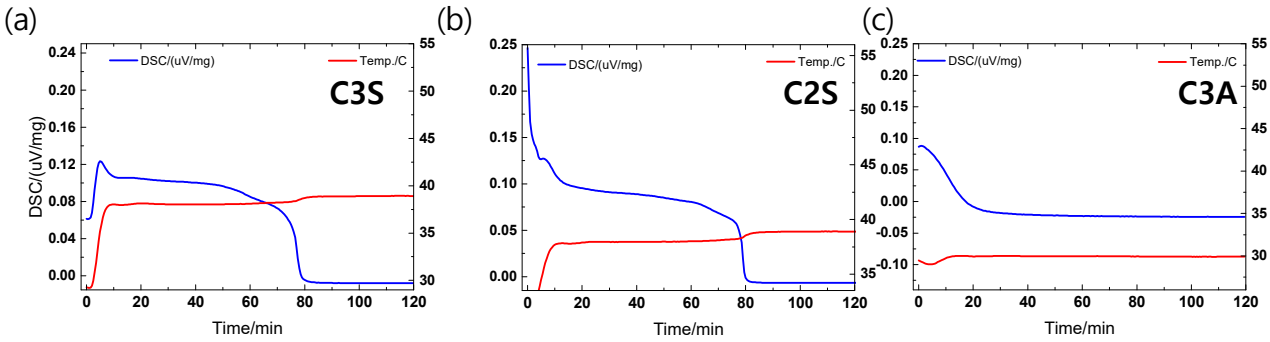

Figure 3. Heat flow (blue line) and cumulative heat (red line) of synthesized C3S, C2S, and C3A powders.

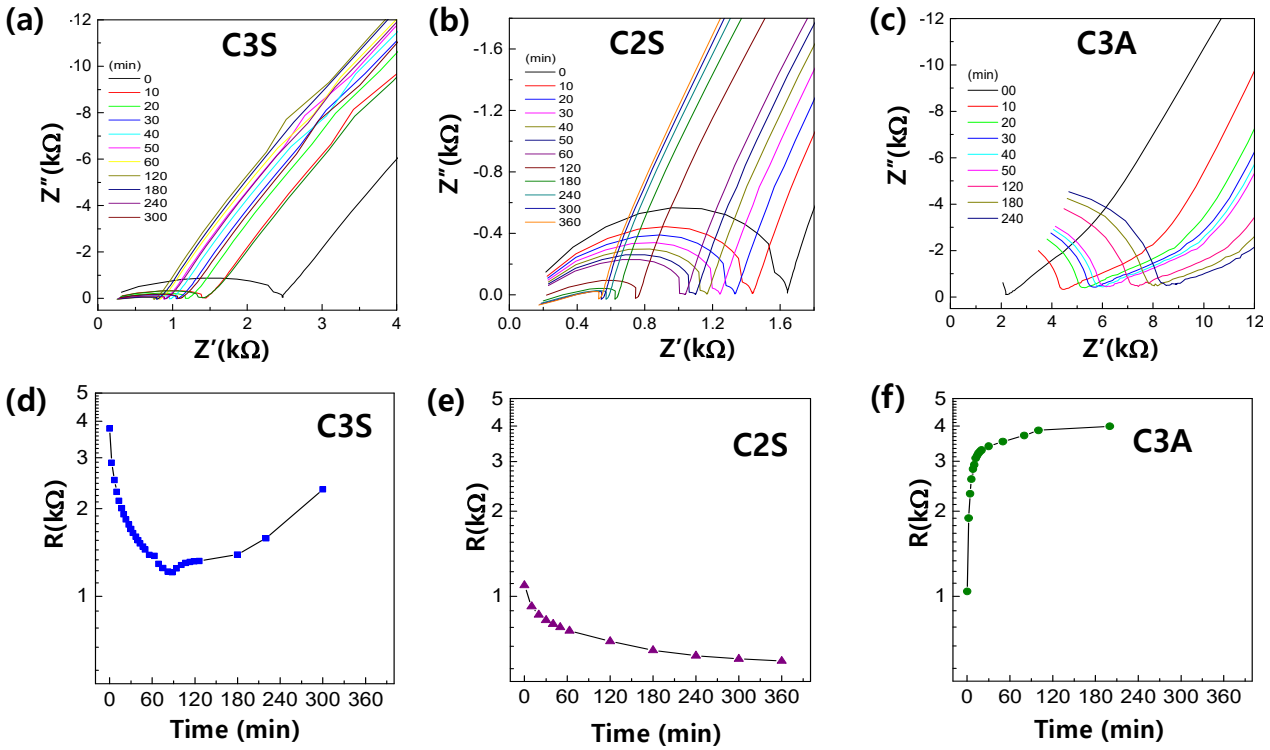

Figure 4. Impedance measurement results (a-c) and inferred resistance values (d-f) at different curing ages for C3S, C2S, and C3A.

for long-term structural stability. This thermal behavior also supports the compositional optimization results derived from the Taguchi analysis, where higher C3A content was associated with faster setting times.

3. Electrochemical impedance spectroscopy

Electrochemical impedance spectroscopy (EIS) was employed to monitor the hydration behavior of C3S, C2S, and C3A over time. Figures 4(a)–4(c) display the Nyquist plots of impedance spectra for each component at various hydration times, while Figures 4(d)–(f) present the corresponding resistance values extracted from the high-frequency intercepts. All samples exhibited a characteristic semicircular arc, indicating typical ionic conduction behavior in cement pastes (19, 20).

For C3S, the resistance initially decreased and then

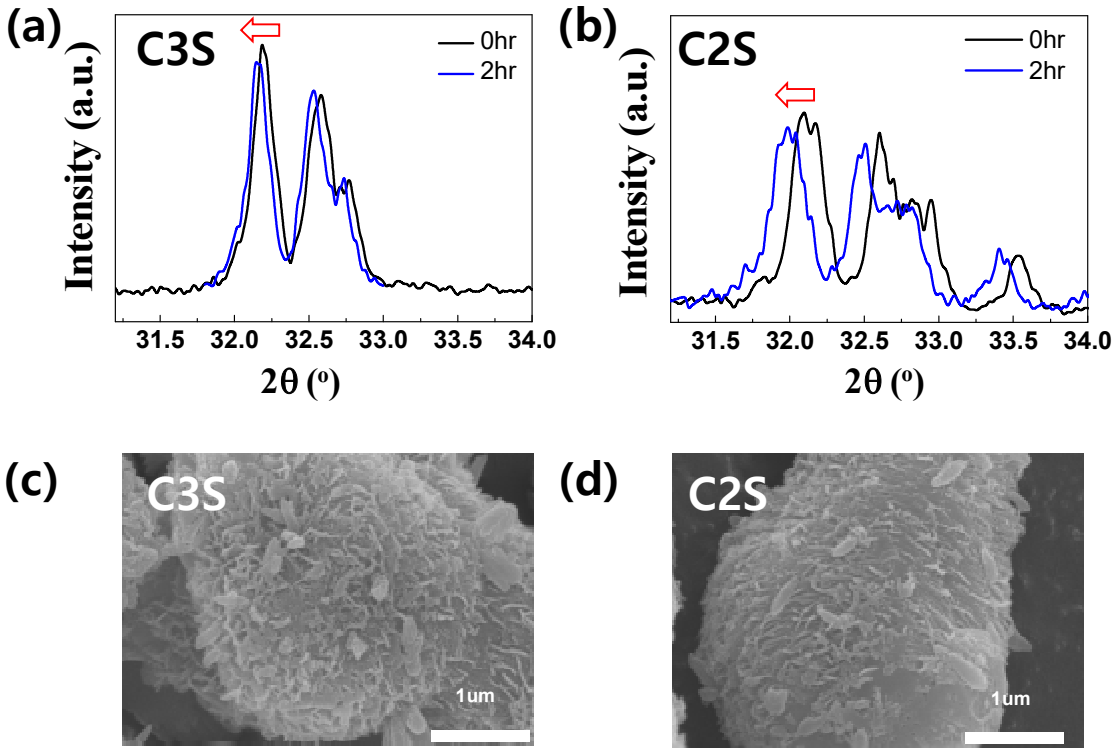

Figure 5. XRD patterns (a, b) and SEM image analysis (c, d) of C3S and C2S after 2 h of hydration.

increased after approximately 60 min. This trend suggests that ionic mobility for dissolved species (e.g., Ca^{2+}, SiO_4^{4-}, OH^-) was initially high due to rapid dissolution, but progressively declined as hydration products, such as calcium silicate hydrate (C–S–H), accumulated and hindered ion transport (21, 22). C2S showed a continuous decrease in resistance throughout the hydration period, indicating a slower but sustained reaction, consistent with its known long-term contribution to strength development. In contrast, C3A exhibited a rapid increase in resistance within the first 20 min, quickly reaching a plateau, reflecting its fast reactivity and early formation of calcium aluminate hydrate (C–A–H). These results clearly demonstrate that electrical resistance is closely correlated with the hydration kinetics of each cement component. The impedance trends also reinforce the findings from DSC analysis, confirming the distinct roles of each phase in controlling the setting behavior of MTA.

4. XRD and SEM analyses for powder hydration

To investigate the phase evolution and morphological changes during hydration, X-ray diffraction (XRD) and scanning electron microscopy (SEM) analyses were conducted on C3S and C2S powders after 2 h of hydration. As shown in the XRD patterns, the main crystalline phases were retained, but the diffraction peaks shifted slightly to lower angles with reduced intensities. This shift indicates lattice expansion due to water absorption during hydration, which is considered beneficial for sealing ability and dimensional stability in clinical applications. The SEM images revealed significant morphological transformation, characterized by the formation of flaky or sheet-like hydration products on the surface of the particles. These structures are indicative of calcium silicate hydrate (C–S–H) and calcium hydroxide (CH) formation, in line with known hydration mechanisms of calcium silicate phases. The

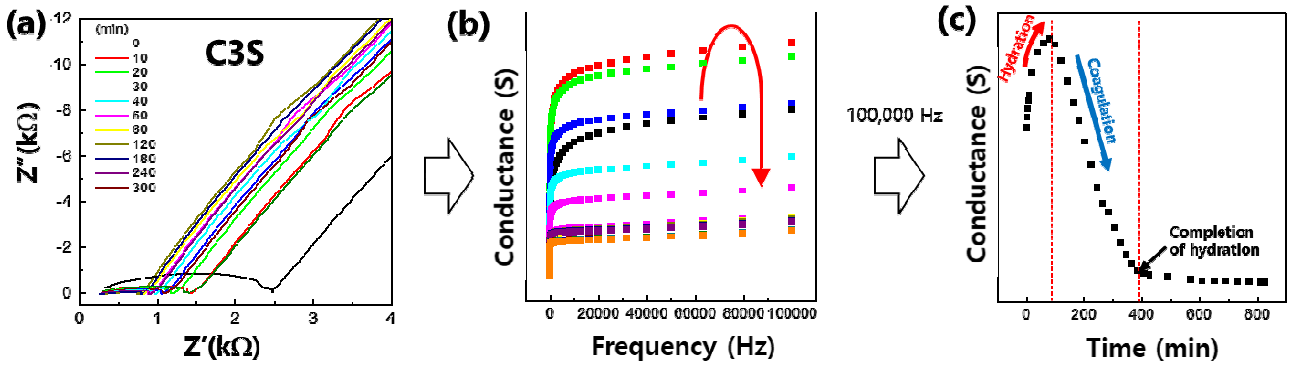

Figure 6. (a) Analysis of the cement hydration process through impedance measurements, (b) conductance changes with frequency, and (c) setting process over time.

Run No.	Factors				Setting time (min)
	A. C2S	B. C3S	C. C3A	D. W/C	
1	1	1	1	1	72
2	1	2	2	2	142
3	1	3	3	3	621
4	2	1	2	3	99
5	2	2	3	2	79
6	2	3	1	1	1789
7	3	1	3	2	85
8	3	2	1	3	1398
9	3	3	2	1	59

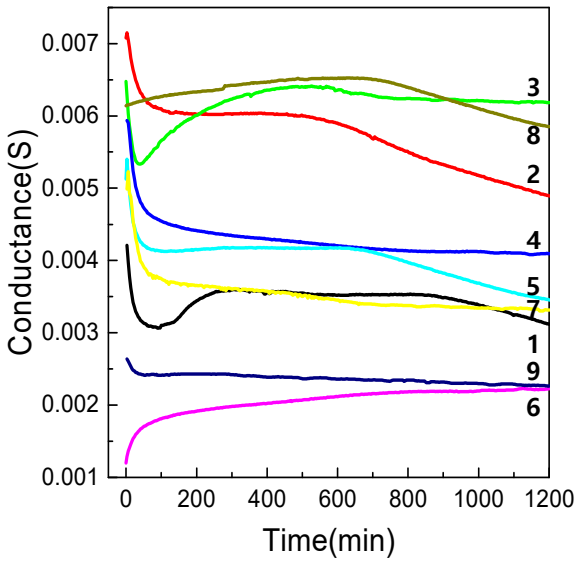

Figure 7. (Experimental results using L9 (34) orthogonal array and impedance measurements.

observed microstructures are consistent with earlier studies, confirming the successful hydration of both C3S and C2S, including the formation and growth of hydration products over time (23).

5. Impedance analysis

To quantify the setting behavior of cement, impedance spectra were further analyzed by converting the data into conductance (S) values across a range of frequencies. As shown in Figure 6(a), raw impedance data were transformed into frequency-dependent conductance curves (Figure 6(b)), allowing for clearer identification of hydration stages. From these data, conductance values at a fixed frequency of 100,000 Hz-where frequency dependence is minimal-were extracted and plotted over time, as shown in Figure 6(c).

The conductance-time profile (Figure 6(c)) revealed three distinct stages in the hydration process: an initial

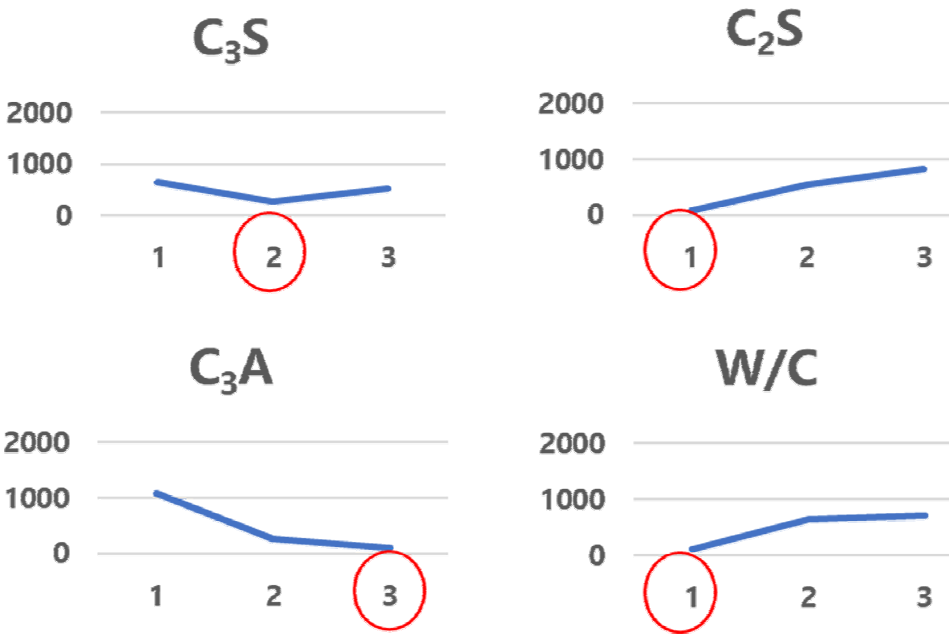

Figure 8. Hydration completion time based on levels of each factor.

increase phase corresponding to ionic dissolution, a rapid decrease indicating the setting point due to the formation of hydration products, and a final plateau phase representing the completion of hydration. This approach enabled precise determination of the setting time for each sample. The analysis demonstrated that impedance-derived conductance is a reliable indicator of the progression of cement hydration, offering a non-destructive, time-resolved method for evaluating material performance.

Discussion

To identify the optimal combination of factors influencing MTA setting behavior, a Taguchi L9 (3^4) orthogonal array was employed using four variables-C2S (A), C3S (B), C3A (C), and water-to-cement (W/C) ratio (D)-each at three levels. The experimental matrix and the corresponding setting times derived from impedance analysis are summarized in Figure 7. Conductance values were tracked over time for each of the nine experimental conditions. The conductance–time curves revealed clear differences in setting behavior depending on the combination of components. Samples containing a higher level of C3A generally exhibited a more rapid decrease in conductance, indicating faster setting due to accelerated hydration. Conversely, higher levels of C2S tended to delay the decrease in conductance, reflecting slower hydration kinetics. The W/C ratio also played a significant role, with lower ratios associated with faster setting due to denser microstructures and limited water availability.

This systematic analysis enabled the identification of an optimal formulation-C3S: level 2, C2S: level 1, C3A: level 3, W/C: level 1-that resulted in the shortest setting time. These results confirm the effectiveness of impedance-based evaluation combined with Taguchi design in optimizing cement formulations.

Figure 8 presents the effect of each experimental factor-C3S, C2S, C3A, and W/C ratio-on the hydration completion time, as determined through Taguchi analysis.

Each factor was tested at three levels, and the mean setting time at each level was calculated based on impedance measurements. The shortest setting time was observed at level 2 for C3S, indicating that a moderate proportion of C3S facilitates balanced hydration and efficient formation of calcium silicate hydrate (C–S–H). For C2S, level 1 resulted in the fastest setting, consistent with its known slower hydration behavior at higher concentrations. In the case of C3A, level 3 exhibited the shortest setting time, confirming that higher C3A content promotes rapid formation of calcium aluminate hydrate (C–A–H) and accelerates the initial setting. Similarly, the W/C ratio showed an optimal value at level 1, where a lower water content likely limited ion mobility but enhanced particle packing, leading to faster setting. Collectively, these results suggest that the optimal formulation for minimizing the hydration setting time comprises C3S at level 2, C2S at level 1, C3A at level 3, and W/C at level 1. This combination yields the fastest setting, as confirmed by both impedance-derived conductance trends and statistical Taguchi analysis, and is consistent with thermochemical behavior observed in previous DSC results.

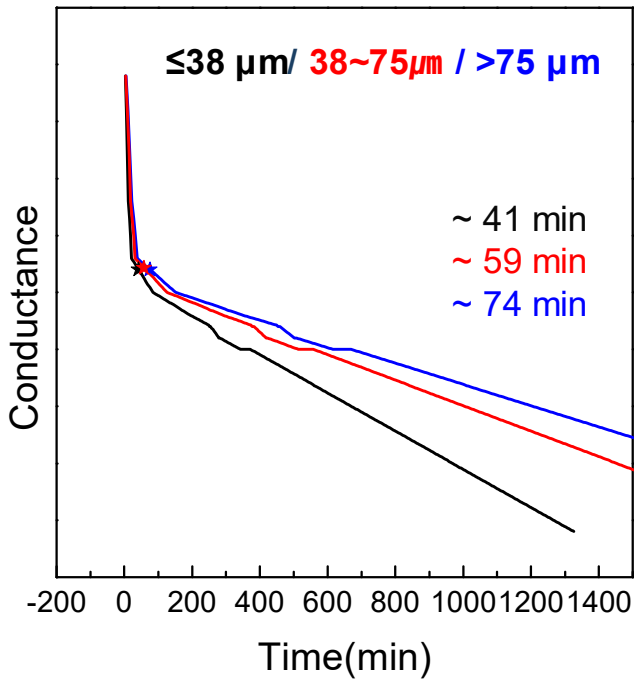

Figure 9. Comparison of MTA setting times based on particle size.

To further assess the effect of physical properties on cement performance, the optimized MTA composition (C3S: 2, C2S: 1, C3A: 3, W/C: 0.3) was sieved into three distinct particle size ranges: ≤38 μm, 38–75 μm, and >75 μm. Figure 9 shows the setting behavior of each group, monitored using impedance-based conductance analysis. The finest particle group (≤38 μm) exhibited the fastest setting time, completing hydration in approximately 41 min. In comparison, the 38–75 μm group set in about 59 min, while the >75 μm group required approximately 74 min to complete hydration. This trend clearly demonstrates that smaller particle sizes significantly accelerate the setting process, likely due to their increased surface area and reactivity, which enhance water penetration and ion exchange during hydration (24, 25).

These findings are consistent with cement chemistry principles and prior thermal and impedance analyses, further validating the role of particle size in optimizing MTA performance. The results suggest that controlling particle size distribution is an effective strategy for tuning setting characteristics in clinical applications. The particle size classification in this study was based on the practical limitations of ball milling and sieving techniques. In future studies, additional work with smaller particles obtained by jet milling and particle size selector should be employed to further optimize MTA properties.

These findings underscore the effectiveness of combining the Taguchi method with impedance analysis as a systematic approach to optimize MTA formulation. In particular, the integration of compositional design and particle size control provides a practical strategy to enhance setting performance. Future studies should aim to validate the clinical applicability of the optimized MTA and explore further functional modifications to expand its utility in dental materials.

Conclusion

This study successfully optimized the setting time of mineral trioxide aggregate (MTA) using the Taguchi method, focusing on the key components tricalcium silicate (C3S), dicalcium silicate (C2S), and tricalcium aluminate (C3A). The synthesized compounds were systematically characterized using XRD, SEM, and DSC analyses. XRD analysis confirmed the single phases of the synthesized compounds, while SEM images showed irregular plate-like structures with particle sizes below 30 μm. DSC analysis demonstrated prolonged exothermic behavior for C3S and C2S, whereas C3A exhibited a rapid thermal response within the first 20 min. Impedance analysis further elucidated the hydration behavior of each component: C3S showed an initial resistance drop followed by an increase, C2S exhibited a gradual resistance decrease, and C3A displayed a rapid resistance rise, reflecting their respective hydration kinetics. The optimized cement composition (C3S:2, C2S:1, C3A:3, and W/C:0.3) was evaluated across three particle size ranges (≤38 μm, 38–75 μm, >75 μm), confirming that smaller particles significantly accelerated the setting process. The final optimized formulation achieved a setting time of approximately 41 min. These results offer an effective approach for tailoring MTA formulations and provide foundational data for the development of high-performance dental cements with improved clinical usability.

Acknowledgements

This research was supported by the National Research Foundation of Korea (NRF) funded by the Korea government (MSIT) (RS-2019-NR040056) and by Chonnam National University (Grant No. 2025-0397-01).

References

1. Pitt Ford TR, Torabinejad M, Abedi HR, Bakland LK, Kariyawasam SP. Using mineral trioxide aggregate as a pulp-capping material. J Am Dent Assoc. 1996;127 (10):1491-4.
2. Nabeel M, Abu Seida AM, Elgendy AA, Tawfk HM. Biocompatibility of mineral trioxide aggregate and biodentine as root-end filling materials: an in vivo study. Sci Rep. 2024;14(1):3568.
3. Pushpalatha C, Dhareshwar V, Sowmya SV, Augustine D, Vinothkumar TS, Renugalakshmi A, et al. Modified mineral trioxide aggregate - a versatile dental material: an insight on applications and newer advancements. Front Bioeng Biotechnol. 2022;10:941826.
4. Camilleri J. Mineral trioxide aggregate: present and future developments. Endod Top. 2015;32(1):31-46.
5. Torabinejad M, Watson TF, Pitt Ford TR. Sealing ability of a mineral trioxide aggregate when used as a root end filling material. J Endod. 1993;19(12),591-5.
6. Main C, Mirzayan N, Shabahang S, Torabinejad M. Repair of root perforations using mineral trioxide aggregate: a long-term study. J Endod. 2004;30(2): 80-3.
7. Ahmed HMA, Luddin N, Kannan TP, Mokhtar KI, Ahmad A. Chemical analysis and biological properties of two different formulations of white portland cements. Scanning. 2016;38(4):303-16.
8. Tawil PZ, Duggan DJ, Galicia JC. MTA: a clinical review. Compend Contin Educ Dent. 2015;36(4):247.
9. Asgary S, Parirokh M, Eghbal M, Stowe S, Brink F. A qualitative X-ray analysis of white and grey mineral trioxide aggregate using compositional imaging. J Mater Sci Mater Med. 2006;17(2):187-91.
10. Gandolfi MG, Sauro S, Mannocci F, Watson TF, Zanna S, Capoferri M, et al. New tetrasilicate cements as retrograde filling material: an in vitro study on fluid penetration. J Endod. 2007;33(6):742-5.

11. Kim M, Yang W, Kim H, Ko H. Comparison of the biological properties of ProRoot MTA, OrthoMTA, and Endocem MTA cements. J Endod. 2014;40(10): 1649-53.
12. Saghiri MA, Kazerani H, Morgano SM, Gutmann JL. Evaluation of mechanical activation and chemical synthesis for particle size modification of white mineral trioxide aggregate. Eur Endod J. 2020;5(2):128-33.
13. Taguchi G, Yokoyama Y. Taguchi methods: design of experiments. Dearborn (MI): Amer Supplier Inst; 1993.
14. Powder Diffraction File. Search manual. PDF-2 release. Pennsylvania (PA): Int Centre for Diffraction Data; 2004.
15. Lim J, Guk JG, Singh B, Hwang YC, Song SJ, Kim HS. Investigation on hydration process and biocompatibility of calcium silicate-based experimental portland cements. J Korean Ceram Soc. 2019;56(4): 403-11.
16. Scrivener K, Snellings R, Lothenbach B, editors. A practical guide to microstructural analysis of cementitious materials. Boca Raton (FL): CRC Press; 2016.
17. Goñi S, Puertas F, Hernández MS, Palacios M, Guerrero A, Dolado JS, et al. Quantitative study of hydration of C3S and C2S by thermal analysis. J Therm Anal Calorim. 2010;102(3):965-73.
18. Kirchheim AP, Rodríguez ED, Myers RJ, Gobbo LA, Monteiro PJM, Dal Molin DCC, et al. Effect of gypsum on the early hydration of cubic and Na-doped orthorhombic tricalcium aluminate. Materials. 2018;11(4):568.
19. Wang R, He F, Shi C, Zhang D, Chen C, Dai L. AC impedance spectroscopy of cement-based materials: measurement and interpretation. Cem Concr Compos. 2022;131:104591.
20. Hu X, Shi C, Liu X, Zhang J, de Schutter G. A review on microstructural characterization of cement-based materials by AC impedance spectroscopy. Cem Concr Compos. 2019;100:1-14.
21. Zhang J, Zheng F, Liu Z, Hong S, Dong B, Xing F. Nondestructive monitoring on hydration behavior of cement pastes via the electrochemical impedance spectroscopy method. Measurement. 2021;185: 109884.
22. Seong KP, Jeon SY, Singh B, Hwang JH, Song SJ. Comparative study of an experimental portland cement and ProRoot MTA by electrochemical impedance spectroscopy. Ceram Int. 2014;40:1741-6.
23. Hu Q, Li Z, Li W, Provis JL, Wang H. Direct three-dimensional observation of the microstructure and chemistry of C3S hydration. Cem Concr Res. 2016;89:170-9.
24. Ha WN, Bentz DP, Kahler B, Walsh LJ. D90: the strongest contributor to setting time in mineral trioxide aggregate and portland cement. J Endod. 2015;41(7): 1146-50.
25. Pushpalatha C, Dhareshwar V, Sowmya SV, Augustine D, Vinothkumar TS, Renugalakshmi A, et al. Modified mineral trioxide aggregate—a versatile dental material: an insight on applications and newer advancements. Front Bioeng Biotechnol. 2022;10:941826.

Original Article

Optimization of mineral trioxide aggregate formulation using Taguchi design and impedance analysis

Mi-Kyung Han[1], Sun-Ju Song[2], Yeong-Joon Park[1,]*

[1]*Department of Dental Materials, School of Dentistry, Chonnam National University, Gwangju 61186, Korea*
[2]*Department of Materials Science and Engineering, Chonnam National University, Gwangju 61186, Korea*

This study aimed to optimize the composition of mineral trioxide aggregate (MTA) to improve its setting time and handling characteristics by applying the Taguchi L9 (3^4) orthogonal array design. The primary components of MTA—tricalcium silicate (C3S), dicalcium silicate (C2S), tricalcium aluminate (C3A)—were synthesized using a solid-state reaction method. The synthesized powders were characterized by X-ray diffraction (XRD), scanning electron microscopy (SEM), and differential scanning calorimetry (DSC) to confirm their phase purity and microstructural features. To assess the influence of composition and water-to-cement (W/C) ratio on setting behavior, electrochemical impedance spectroscopy (EIS) was performed to monitor hydration progression in real time. The Taguchi method enabled the assessment of four factors (C3S, C2S, C3A, and W/C ratio) at three levels each, identifying the optimal formulation: C3S:2, C2S:1, C3A:3, and W/C:0.3. The cement prepared under these conditions was further sieved into three particle size ranges (≤38 μm, 38–75 μm, >75 μm) to analyze the effect of particle size on setting performance. The finest particle group exhibited the shortest setting time of 41 min. DSC and impedance results confirmed that smaller particle sizes and optimized composition promoted more efficient hydration. This study demonstrates that the combination of Taguchi design and impedance analysis offers an effective strategy for optimizing MTA formulations. The findings contribute to the development of high-performance dental cements with faster setting times and improved clinical usability.

Keywords : Mineral trioxide aggregate (MTA), Taguchi method, Impedance analysis, Setting time